



Sedimentology and geochemistry of the Kavakköy Travertine (Konya, central Turkey)

Seda Karaisaoğlu¹ · Hükmü Orhan¹

Accepted: 4 February 2018 / Published online: 12 February 2018
© Springer-Verlag GmbH Germany, part of Springer Nature 2018

Abstract

In the Kavakköy region located at Southwest of Konya (central Turkey), four Quaternary travertine mounds and two recent travertine deposition sites are roughly aligned along the Seydişehir Fault Zone. Water temperature of recent travertine sites is about 39 and 19 °C. Six different facies were determined from the Kavakköy Travertine: crystalline crust travertine, paper-thin raft travertine, coated bubble travertine, pisoid, lithoclast travertine and shrub travertine facies. Sedimentological, morphologic and geochemical characteristics of these facies point toward depositions in slope and depressional depositional systems. Rare element content and isotopic values of different facies are distributed on diagrams as two separate clusters. After comparing with two recent travertines, it is hypothesized that they are most probably related to the temperatures of travertine formation water. High $\delta^{13}\text{C}$ contents and calculated $\delta^{13}\text{C}$ values, using Panichi and Tongiorgi's (in: Proceedings of the 2nd UN symposium on the development and use of geothermal resources, San Francisco, CA, 20–29 May 1975, pp. 815–825, 1976) equation, imply that parent water was charged with CO_2 from a deep origin. Significant differences in the $\delta^{13}\text{C}$ and $\delta^{18}\text{O}$ isotopic values of recent travertines at two different sites have been interpreted as being related to water circulation path and source of CO_2 . The travertine precipitated by water with a temperature of 19 °C has comparatively short and shallow fluid flow paths and low (normal) heat flow and has CO_2 isotopic signatures, indicating a comparatively large quantity of CO_2 contribution from decarbonation of limestone. In contrast, the travertine formed by relatively hot water (39 °C) had been conductively heated during percolating through thick Paleozoic–Cenozoic sequence and has incorporated a comparatively large quantity of CO_2 derived from mantle sources.

Keywords Travertine · Kavakköy · Quaternary · Stable isotope

Introduction

Travertine is a continental carbonate rock deposited around the springs having water rich in Ca and bicarbonate (Guo and Riding 1998). Pentecost (2005) classified fresh water carbonates into two groups: “thermogene carbonates”, which are formed from hot water and “meteogene carbonates”, which are formed from cold water. Many authors have accepted that travertine is derived from hot water (Chafetz and Lawrence 1994; Altunel 1996; Guo and Riding 1998; Fouke et al. 2000; Özkul et al. 2002, 2013; Koşun 2012). Travertine is hard, crystalline, generally laminated and less porous carbonates. On the other hand,

tufa is cold water carbonate. It is generally highly porous and contains higher plant and animal remains (Pedley 1990; Ford and Pedley 1996; Guo and Riding 1998). Travertine deposits are commonly associated with normal or transtensional faults (Altunel 1996; Hancock et al. 1999; Brogi and Capezzuoli 2009; Özkul et al. 2013) as they are in this study. The depositional architecture, geochemical characteristics and precipitation of travertine are mainly controlled by (i) mechanical factors such as the pCO_2 of the spring water when discharged at its vent (Herman and Lorah 1987; Lorah and Herman 1988; Chafetz and Lawrence 1994; Barilaro 2012); (ii) the area and depth of water on the discharge apron (Dandurand et al. 1982; Barilaro 2012); (iii) the amount of water agitation and turbulence (Jacobson and Usdowski 1975; Lorah and Herman 1988; Barilaro 2012); (iv) aeration, jet-flow, and low-pressure effects (Zhang et al. 2001; Barilaro 2012), increasing temperature and evaporation and biological factors such as

✉ Seda Karaisaoğlu
s.karaisaoğlu@gmail.com

¹ Department of Geological Engineering, Faculty of Engineering, Selçuk University, Selçuklu, Konya, Turkey

photosynthetic CO₂ uptake and other physiological activities of plants, bacteria living in hot water (Barilaro 2012); (v) climate, spring water composition and (vi) the source of CO₂.

Different travertine facies have been determined at different geographic settings and depositional environments (Chafetz and Folk 1984; Guo and Riding 1998; Minissale et al. 2002; Özkul et al. 2002; Pentecost 2005; Rainey and Jones 2005; Gandin and Capezzuoli 2008; Kele et al. 2011; Barilaro 2012; Koşun 2012). To find which factors were influential may be achieved by comparing recent spring deposits at differing geological settings.

This study describes and elucidates the depositional, mineralogical, and geochemical characteristics of four Quaternary travertine mounds and two recent travertine sites around Kavakköy (Konya, central Turkey) with the view of establishing factors that controlled their development. The data obtained from this study will be used in evaluating similar deposits throughout the World.

Geological setting

The study area is located at southwest of Kavakköy, 15 km to north of Seydişehir (Konya, central Turkey; Fig. 1). The Early–Middle Cambrian Çaltepe Formation is the oldest unit in the study area and comprises weakly metamorphosed recrystallized limestone and dolomite. The Seydişehir Formation, which rests conformably on the Çaltepe Formation, is Late Cambrian–Early Ordovician in age and is represented by alternated metasandstone, shale and phyllite. The Triassic–Lower Cretaceous carbonates come unconformable on these units (Özgül 1976). The Miocene–Pliocene volcanic rocks are andesitic–basaltic in character and cover a large area at the eastern site of the study area (Fig. 1; İnnocenti et al. 1975). The Neogene Taşlıca Formation lies unconformably on the above-mentioned units and comprises highly fossiliferous, fractured thin-bedded limestone and weakly consolidated sandstone, mudstone and marl. Quaternary travertines occur as mounds, which are roughly aligned in a row along the Seydişehir Fault Zone. Recent travertine

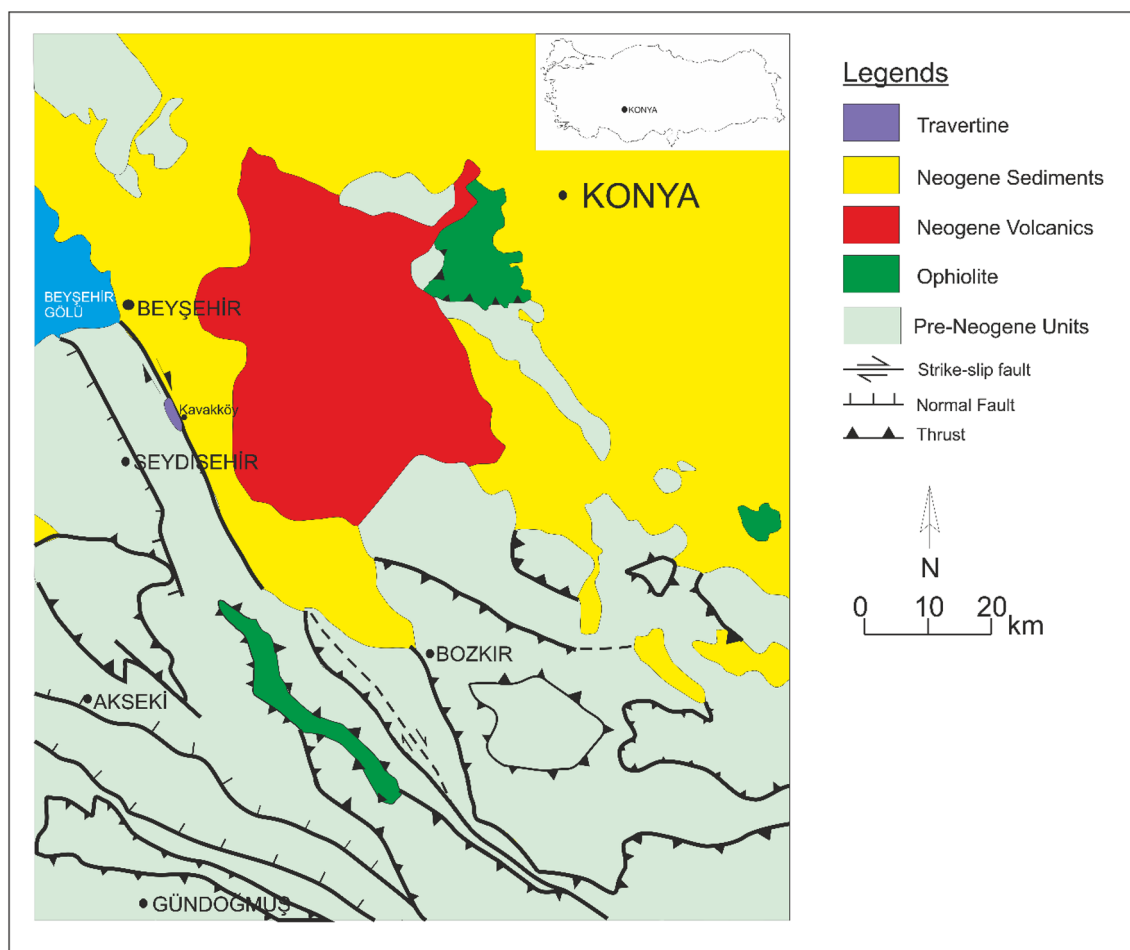


Fig. 1 Simplified geological map of the study area. Modified after Özgül (1997)

deposition is taking place around the output of an artificial artesian well (230 m deep) and a spring located 2 km further. The temperature and the pH of the well and spring water are 39 °C; 6.51 and 19 °C; 6.41, respectively.

The Bozkır and Hadım nappes formed in relation to the closing of the Neo-Tethys ocean as well as the Seydişehir Fault Zone (SFZ) developed during the neo-tectonic period are the main tectonic features in the study area (Özgül 1976, 1997; Koçyiğit 1984). The Seydişehir Fault Zone extending NW–SE in the study area can be followed for 7–8 km and it cut across travertine mounds around Kavakköy (Fig. 1).

Methods

The sedimentological characteristics and lateral–vertical relations of travertine and tufa (?) facies were determined during field studies by recognizing the characteristics introduced by Guo and Riding (1998). Systematic samples were collected from all travertine facies in quarries (Fig. 2a) opened on travertine mounds for mineralogical, petrographical, geochronologic and geochemical evaluation. The temperature and pH of two water outlets in the study area were measured by means of Hanna Combo pH&EC instruments and recent tufa deposits were also sampled (Fig. 2b).

Of 104 samples, 23 samples were subjected to elemental analysis, 56 samples for stable isotope analysis, 3 samples for U-Th dating and 83 samples for XRD analysis. Scanning electron microscope investigations were performed on gold coated samples using a “Zeiss evo Is 10” microscope. Mineralogical compositions of the randomly oriented powdered travertine samples were determined by X-ray powder diffraction (XRD) technique using a Bruker D-8 Advance diffractometer with CuK α radiation at 40 kV and 40 mA. The SEM and XRD analyses were performed at the ILTEK center of Selcuk University, Konya, Turkey. Stable carbon and oxygen isotope measurements of the travertines and four

water samples were performed at the Institute for Geological and Geochemical Research Institute, Hungarian Academy of Sciences, Budapest, Hungary. Carbon and oxygen isotope analyses of bulk travertine samples were carried out using both the conventional phosphoric acid method (H₃PO₄ digestion method at 25 °C) of McCrea (1950) and the continuous flow technique of Spötl and Vennemann (2003). $\delta^{18}\text{O}$ analysis of waters was conducted using the CO₂–water equilibration method of Epstein and Mayeda (1953). All samples were measured at least in duplicate and the mean values are given in the standard δ notation in parts per thousand (‰) relative to Vienna Pee Dee Belemnite (VPDB; $\delta^{13}\text{C}$ and $\delta^{18}\text{O}$) and Vienna Standard Mean Ocean Water (VSMOW). 50–100 mg of gently crushed, ultrasonically treated and dried three samples, which were chosen among compact, light colored and primarily deposited samples, were subjected to U-Th dating analysis (Shen et al. 2012) at the High-precision Mass Spectrometry and Environment Change Laboratory (HISPEC), Department of Geosciences, National Taiwan University, Taipei, Taiwan.

Facies of the Kavakköy Travertine

Travertine facies and their depositional environments have been defined by many scientists from different parts of the world and in different geological settings (Chafetz and Folk 1984; Guo and Riding 1998; Minissale et al. 2002; Özkul et al. 2002, 2013, 2014; Pentecost 2005; Rainey and Jones 2005; Gandin and Capezzuoli 2008; Kele et al. 2011; Koşun 2012; Orhan and Kalan 2015). Six different facies based on Guo and Riding (1998) classification were determined in the Kavakköy Travertine.

Crystalline crust facies

This facies is made up of a few millimeters to centimeter thick layers of coarse radial calcite crystals which were



Fig. 2 **a** A travertine quarry in the Quaternary travertine mound and **b** artesian well in the study area

oriented with their long axis perpendicular to the growing surface. It is white and compact and has a few tens of meters of lateral continuity. Its thickness is in the range of 80–115 cm. Vertically elongated voids were observed in some levels (Fig. 3a). Microscopic analysis reveals that the crystalline crust facies is formed by finely laminated dendritic architectures exhibiting, in general, well-developed fan-shaped morphologies (Fig. 3b, c).

Interpretation: Crystalline crust facies develops on a low to high angle, mainly with dips of $10^\circ \pm 4^\circ$, non-terraced smooth slopes and reflects that deposition took place in an agitated and rapidly flowing water (Guo and Riding 1998). Thick layers of crystalline crust represent fast deposition in relatively fast flowing water and thin layers represent slow precipitation in a relatively slow flow (Folk et al. 1985; Guo and Riding 1992, 1998; Özkul et al. 2002, 2014; Jones and Renaut 2010).

Raft facies

Paper-thin raft facies is characterized by white to cream colored, thin, delicate, brittle and flat crystalline layers. Raft

deposits are often associated with the coated bubble facies (Fig. 4a). Recent raft formations were observed on the surface of pool water in the study area (Fig. 4b).

Interpretation: Paper-thin rafts, also known as “hot water ice” (Allen and Day 1935) and “calcite ice” (Bargar 1978), are developed on the surface of stagnant water bodies where surface degassing of CO_2 causes an increase in saturation *re* CaCO_3 leading to calcite or aragonite precipitation (Baker and Fiosticks 1951; Folk et al. 1985; Chafetz et al. 1991; Guo and Riding 1998; Özkul et al. 2002). They generally occur as a few individual sheets but locally they are found as dense concentration by accumulations on the floor of small stagnant pools and as sheets of still water (Guo and Riding 1998; Barilaro 2012).

Coated bubble facies

The coated bubble facies consists of sub-spherical to circular or elongated micritic/microsparitic coatings around porous structures with a diameter ranging from 2 mm to 2 cm (Fig. 5a). Some of gas hollows are filled with sparitic

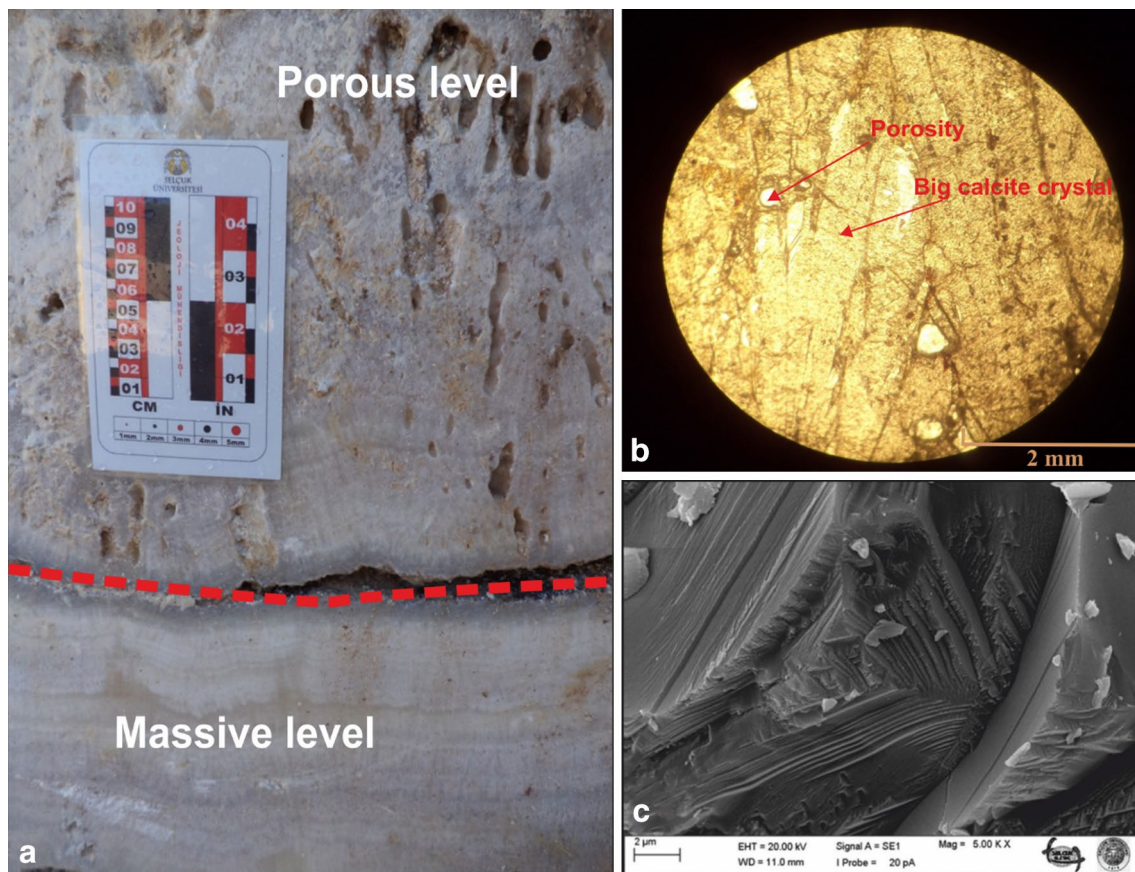


Fig. 3 a Crystalline crust facies: field appearance of dense and porous crystalline crust facies, b crossed polarized light photomicrograph and c SEM image of dense crystalline crust exhibiting strong crystalline habit and fan-shaped morphology

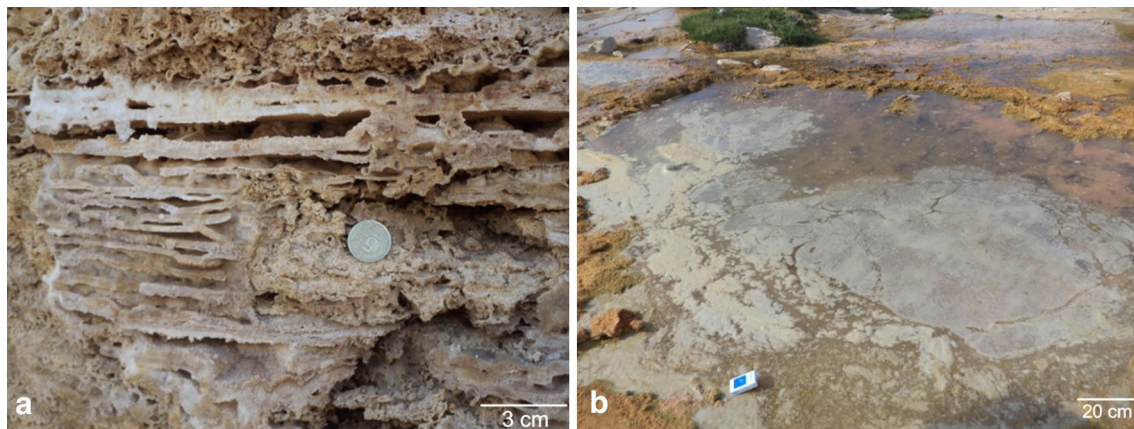


Fig. 4 **a** Quaternary rafts facies-associated coated gas bubbles and **b** recent rafts on the surface of a stagnant water body in the study area

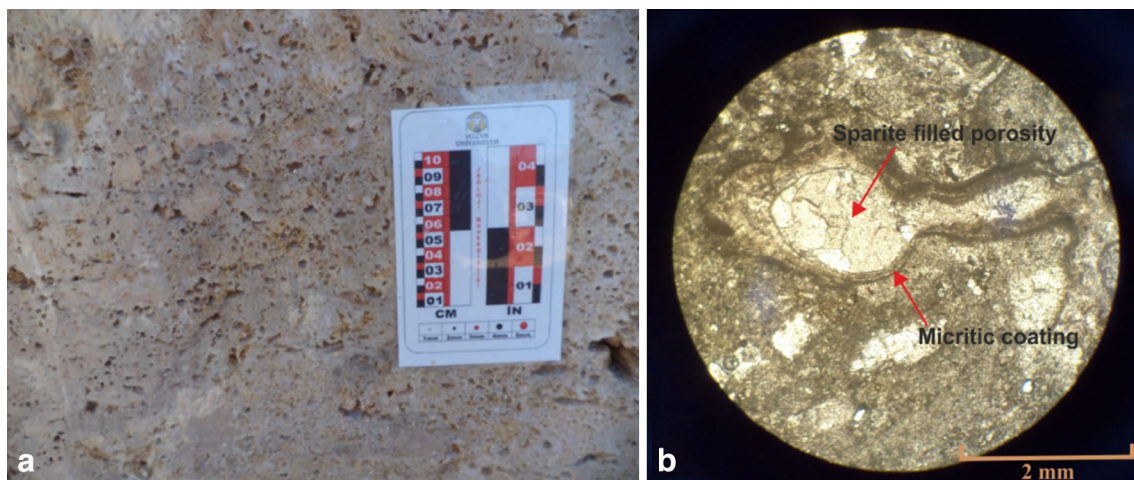


Fig. 5 **a** Coated bubble facies; field appearance and **b** Crossed polarized light photomicrograph showing bubble-coated facies consisting of sub-spherical to circular porous structures coated by micrite layers. Some of pores were filled by blocky sparite

calcite (Fig. 5b). This facies is generally observed beneath the raft facies.

Interpretation: Coated bubbles mainly form in places, such as near pool surfaces below paper-thin rafts, or among crystals or vegetation in pools and porous sediments, where bubbles are trapped (Guo and Riding 1998; Özkul et al. 2002; Barilaro 2012). The source of these bubbles is mainly from microbial activity in underlying sediments but in some places the degassing of the water near its outlet produces bubbles as it was seen in the study area.

Pisoid facies

This facies comprises white or pale yellow pisoids ranging in shape from spherical to irregularly rounded and varies in size from a few millimeters to 2 cm (Fig. 6a). Recent pisoids are present in small pool of micro terrace (Fig. 6b).

Generally, they have a sparitic core and concentrically laminated micrite/sparit interlaminae (Fig. 6c). They are either loose or consolidated with micrite (Fig. 6d) and show very little abrasion.

Interpretation: Pisoids in a travertine may form as (1) concentrically laminated grains (Folk and Chafetz 1983); (2) dendroids (Folk and Chafetz 1983); and (3) stromatolitic mammillate (Guo and Riding 1998). The concentrically laminated pisoids present in the study area have been interpreted as being formed in splashing and turbulent water and have been regarded as inorganic precipitates (Folk and Chafetz 1983; Guo and Riding 1998; Barilaro 2012).

Lithoclast facies

Lithoclast travertine facies is interbedded with other light colored facies (Fig. 7a) and comprises light colored clasts

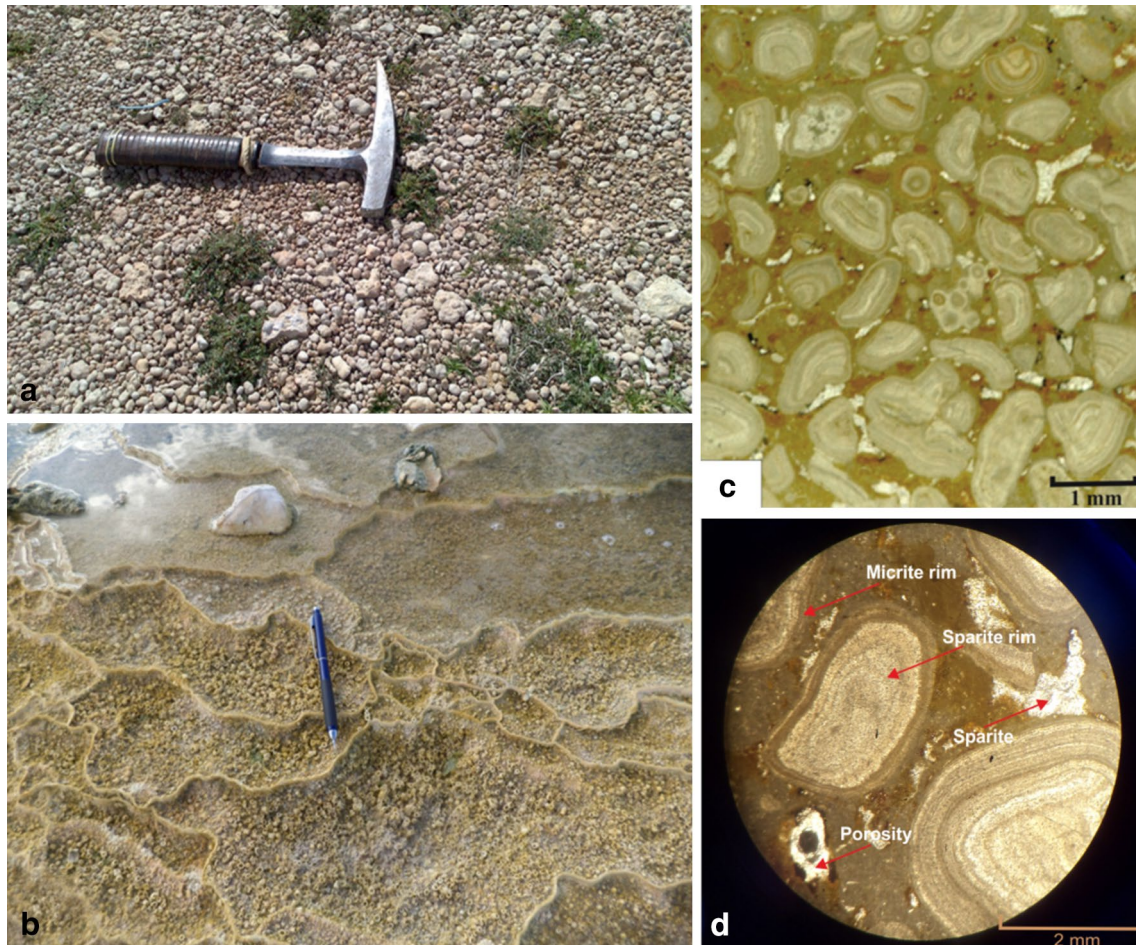


Fig. 6 Pisoid travertine facies. **a** Recent pisoids precipitated by splashing water around the artesian well; **b** recent pisoids depositing in micro terraces (pen is 12 cm); **c** acetate peel and; **d** thin section image of concentrically laminated pisoids with different size

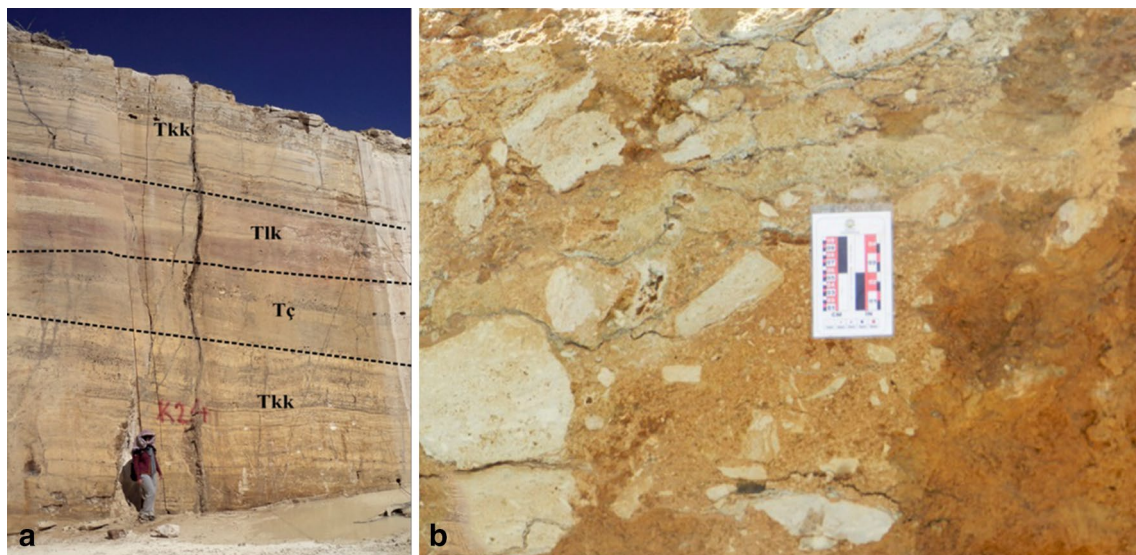


Fig. 7 **a** Field photographs of horizontally bedded travertines facies (Tkk: crystalline crust facies, Tc: shrub facies and Tlk: lithoclast facies) and **b** close view of lithoclast facies

of travertine, mainly from crystalline crust facies (Fig. 7b), mixed with a dark orange to brown colored micritic matrix. It has a thickness ranging from 20 cm to 1 m.

Interpretation: Lithoclast travertine facies develops either as a result of penecontemporaneous erosion of slope travertines and deposition of fragments from terrace rims or collapsed crystalline travertine on the lower slopes and depressions, where it mixes with in situ precipitates, or as a result of the collapse of low cliffs, as in waterfalls (Chafetz and Folk 1984; Casanova 1986; Pentecost 1990; Guo and Riding 1994, 1998).

Shrub facies

This facies is characterized by small shrub-like growth. Shrubs are a few millimeters to a few centimeters in size, white to gray in color and, show a dendritic morphology with vertically aligned calcite crystals (Fig. 8a). It occurs typically as several layers, 1–3 cm thick, which are separated by thin micritic laminae (Fig. 8b).

Interpretation: Three types of shrubs were defined by Chafetz and Guidry (1999). *Bacterial shrubs* have highly irregular forms, while *crystal shrubs* and *ray crystal crusts* display regular geometric patterns. They interpreted that the bacterial and crystal shrubs are bacterially mediated, while ray crystal crusts are formed by a combination of bacterial and abiotic processes. Shrub travertine facies in the study area has been interpreted as crystal shrub and as being deposited in depressions where the water energy is low.

Depositional systems of facies

Three depositional systems for travertine have been introduced by Guo and Riding (1998) for Rapolano Terme travertine in Italy. These depositional systems include (i) the slope

depositional system; (ii) the depression depositional system; and (iii) the Reed mound depositional system.

The sedimentological, morphological and mineralogical characteristics of facies in the Kavakköy Travertine point to the fact that they were developed in slope and depressional depositional systems (Fig. 9). Also, the absence of unconformities and paleosol supports this interpretation.

Travertine geochemistry

Major and trace elements

All facies are almost composed of pure calcite (in XRD analysis, Fig. 10) and contain very little detrital material. The major oxide, trace and rare earth element contents of recent travertine around two water outlets and four Quaternary travertine mounds in the study area are given in Tables 1, 2 and 3. The CaO content of Quaternary travertines ranges between 44.92 and 55.86%, while the content of recent travertines around hot water outlet changes between 52.6 and 54.63% and those around cold water changes between 54.43 and 54.61%. MgO content of the older travertines changes between 0.17 and 0.98% while the MgO of the recent travertines ranges from 0.30 to 0.50% mol.

There are positive correlations between Al_2O_3 , Fe_2O_3 , SiO_2 and total REE contents, whereas there are negative correlations between REE and CaO contents (Fig. 11a–e). Even though trace element contents of different facies are slightly distinctive, there are significant differences in trace elements between recent and older travertines (Table 2).

The results of analyses show no significant differences in the rare earth element content and isotopic values of different facies. But on the diagrams drawn using CaO versus rare earth element content (Sr, Ba, As, Zr, Y, Zn, Rb), two separate clusterings were realized. These groupings are

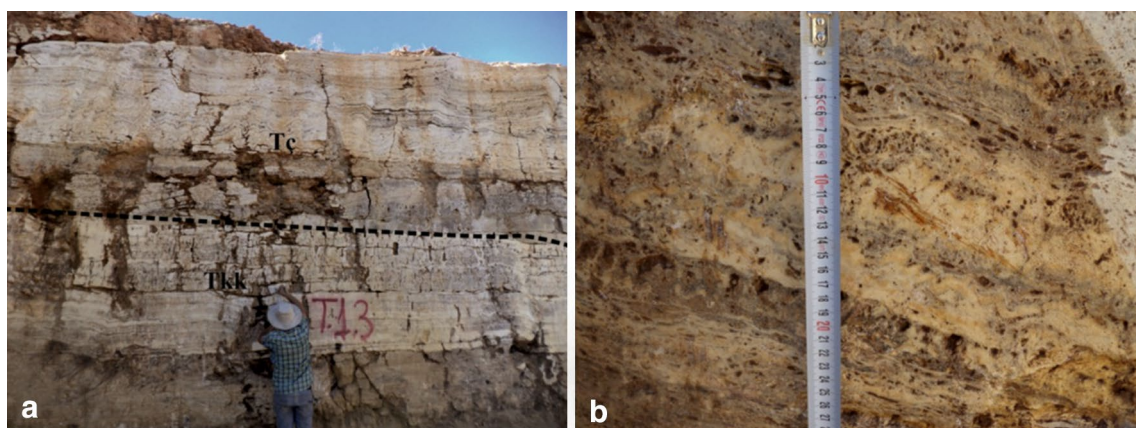


Fig. 8 **a** Field photographs of horizontally bedded travertines facies (Tkk: crystalline crust facies, Tc: shrub facies) and **b** close view of horizontally bedded shrub facies

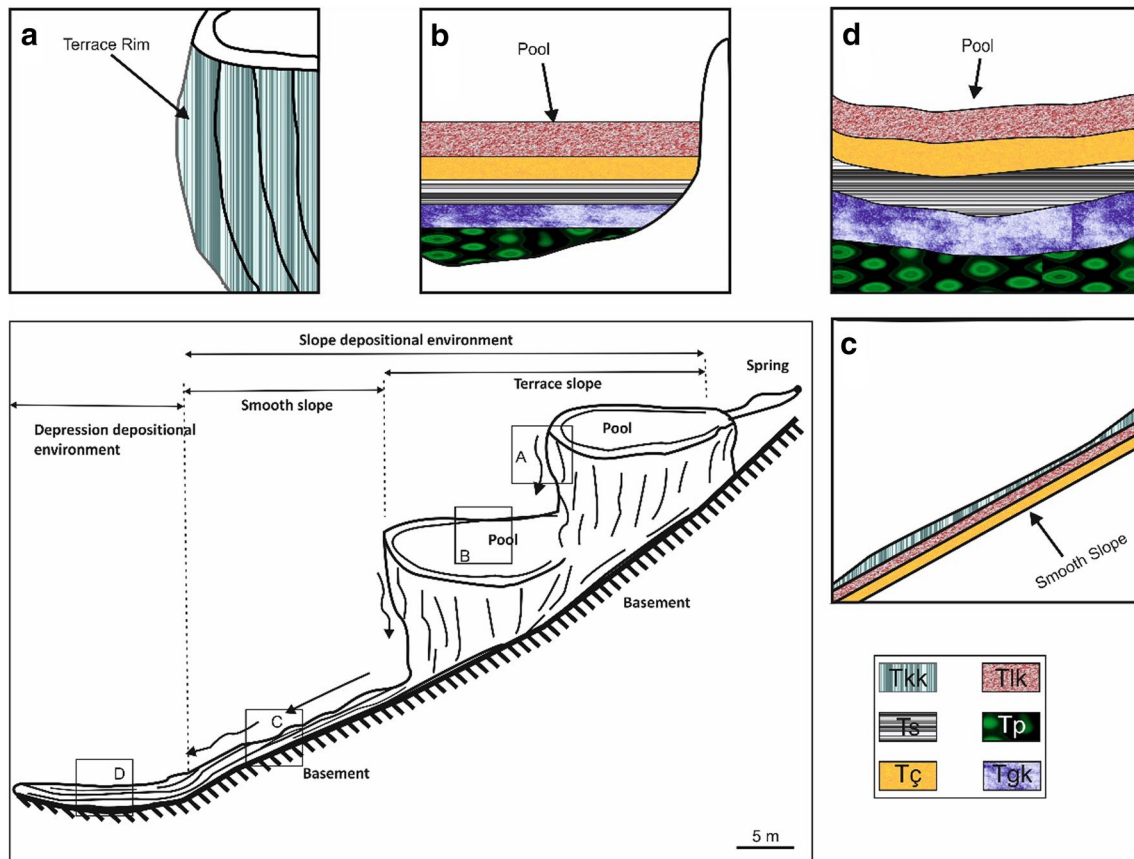


Fig. 9 Depositional model for Kavakköy Travertine (Tkk: crystalline crust facies, Tp: pisoid facies; Ts: raft facies, Tgk: coated bubble facies, Tç: shrub facies, Tlk: lithoclast facies). Adapted from Özkul et al. (2002)

Fig. 10 X-ray diffractogram of travertine samples

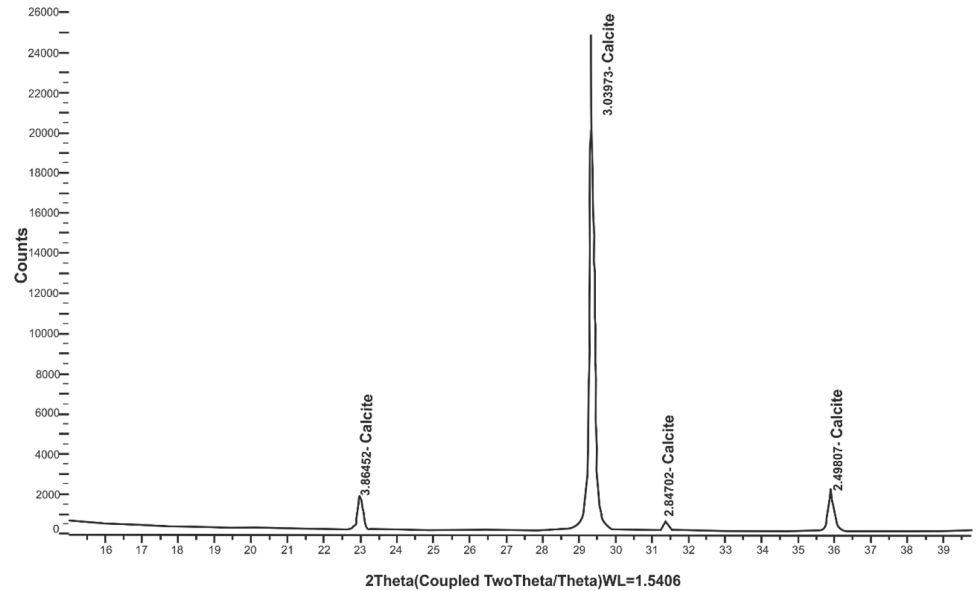


Table 1 Main oxide compositions (in %) of travertine samples from the different facies in the Kavakköy Travertine

Facies type	Sample no.	SiO ₂	Al ₂ O ₃	Fe ₂ O ₃	MgO	CaO	Na ₂ O	K ₂ O	TiO ₂	P ₂ O ₅	MnO	Cr ₂ O ₃	LOI	Total
Crystalline crust facies	SK.48	0.01	0.01	0.06	0.71	55.08	0.02	0.01	0.01	0.01	0.05	0	44	99.9
	SK.74	0.01	0.01	0.06	0.86	55.65	0.02	0.01	0.01	0.01	0.03	0	43.4	99.94
	SK.10	0.01	0.01	0.11	0.9	55.14	0.01	0.01	0.01	0.01	0.08	0	43.8	99.94
	SK.59	0.01	0.01	0.2	0.55	55.19	0.02	0.01	0.01	0.01	0.05	0	44	99.96
	SK.82	0.01	0.01	0.13	0.54	55.16	0.02	0.02	0.01	0.01	0.05	0	44.1	99.95
	SK.1	0.01	0.01	0.24	0.62	54.84	0.02	0.01	0.01	0.01	0.04	0	44.2	99.96
	SK.64	0.01	0.01	0.18	0.6	54.88	0.09	0.02	0.01	0.01	0.02	0	44.2	99.93
	SK.53	0.01	0.01	0.71	0.22	54.83	0.03	0.02	0.01	0.01	0.15	0	44	99.92
Shrub facies	SK.43	0.01	0.01	0.04	0.44	55.86	0.01	0.01	0.01	0.01	0.01	0	43.5	99.83
	SK.76	0.07	0.03	0.11	0.43	55.19	0.01	0.02	0.01	0.01	0.04	0	44	99.89
	SK.26	0.01	0.01	0.15	0.19	56.17	0.01	0.01	0.01	0.01	0.04	0	43.4	99.93
	SK.45	0.15	0.01	0.29	0.17	55.78	0.01	0.01	0.01	0.01	0.23	0	43.4	99.94
	SK.67	0.01	0.01	0.26	0.24	55.33	0.01	0.01	0.01	0.01	0.15	0	44	99.95
Lithoclast facies	SK.7	2.55	0.79	0.46	0.4	52.52	0.03	0.13	0.05	0.02	0.05	0	42.7	99.69
	SK.55	5.74	1.56	1.15	0.39	49.75	0.04	0.24	0.11	0.02	0.05	0	40.9	99.93
Pisoid facies	SK.85	8.94	2.89	1.86	0.92	44.92	0.09	0.48	0.17	0.05	0.26	0.01	39.3	99.85
	SK.86	9.36	2.71	1.71	0.98	44.95	0.09	0.45	0.15	0.08	0.27	0.01	39.1	99.86
Recent hot water trav. sample	SK.40	3.05	0.59	0.36	0.5	52.6	0.16	0.14	0.02	0.01	0.22	0	42.2	99.9
	SK.35	0.47	0.08	0.24	0.51	54.63	0.02	0.01	0.01	0.01	0.18	0	43.8	99.89
Recent cold water trav. sample	SK.68	0.28	0.01	0.31	0.33	54.61	0.01	0.01	0.01	0.01	0.05	0	44.2	99.71
	SK.38	0.36	0.02	0.16	0.5	54.43	0.01	0.01	0.01	0.01	0.04	0	44.3	99.73

interpreted as being most probably related to the temperatures of travertine formation water (Fig. 12a–g).

Stable isotopes

The Quaternary travertine samples in the study area have $\delta^{18}\text{O}$ values ranging from -14.6 and -6.8‰ (VPDB) and recent travertines between -13.5 and -8.7‰ (VPDB); similarly, older travertine samples have $\delta^{13}\text{C}$ values between $+0.2$ and $+8\text{‰}$ (VPDB) and recent travertine between $+5.4$ and $+8\text{‰}$ (VPDB) (Table 4). Based on the $\delta^{13}\text{C}$ and $\delta^{18}\text{O}$ composition (Pentecost 2005; Teboul et al. 2016), the studied travertines are mainly classified as hypogenic travertine. High $\delta^{13}\text{C}$ values imply that the parent water was charged with CO_2 from a deep origin, which is either associated with decarbonation of carbonate resulted from thermal, magmatic and metamorphic processes or with magmatic CO_2 from active volcanism (Kele et al. 2011; Teboul et al. 2016).

Discussion

The sedimentological and mineralogical characteristics of six different facies in the Kavakköy Travertine, which were developed around a water discharge area related to the Seydişehir Fault Zone point that the Kavakköy Travertine

was deposited on a slope and depression depositional setting. Similar interpretation was proposed for Rapolano Terme travertine in Italy (Guo and Riding 1998) and for Pamukale travertine in Denizli, Turkey (Özkul et al. 2002, 2013).

Of the six facies determined from the Kavakköy Travertine, Crystalline crust facies was formed through rapid precipitation at the terrace pool rims and on the slopes where the water flows fast. Paper-thin raft facies and coated bubbles facies were developed on the calm water bodies in terrace pools and depressions. The pisoidic facies was deposited in agitated terrace pools and large depressions with biotic and abiotic processes. Lithoclast travertine facies formed as a result of deposition of fragments broken from terrace rims or collapsed crystalline travertine facies in terrace pools or depressions. The shrub travertine facies is commonly deposited on subhorizontal surfaces on terrace pools, depressions and slope flats (Fig. 9).

Generally, travertine has more positive $\delta^{13}\text{C}$ (VPDB) values, in the range of -1 to 10‰ (Pentecost 2005; Koşun 2012; Özkul et al. 2014), than tufa. Having different isotopic values is acceptable because, in a travertine depositional environment, several differing facies may develop under differing conditions (Özkul et al. 2002). The differences in travertine isotope geochemistry are controlled by physical and chemical processes such as CO_2 degassing, cooling water, evaporation, temperature, saturation, water flow, biological activities and photosynthesis, the origin of CO_2 , type

Table 2 Trace element compositions (in ppm) of travertine samples from the different facies in the Kavakköy Travertine

Facies type	Sample no.	Ba	Be	Co	Cs	Ga	Nb	Rb	Sr	V	W	Zr	Y	Cu	Pb	Zn	Ni	As	
Crystalline crust facies	SK.48	510.00	1.00	0.20	0.10	1.10	0.10	0.10	263.30	8.00	0.50	6.20	0.80	0.50	0.10	1.00	0.10	0.50	
	SK.74	255.00	1.00	0.20	0.10	0.90	0.10	0.10	176.90	8.00	0.80	0.30	0.10	1.40	0.10	1.00	0.10	1.40	
	SK.10	186.00	2.00	0.20	0.10	0.90	0.10	0.10	165.80	8.00	1.30	0.50	0.60	0.80	0.10	1.00	0.50	1.20	
	SK.59	104.00	2.00	0.20	0.10	0.70	0.10	0.10	149.10	8.00	5.60	0.30	0.10	0.20	0.10	1.00	0.10	5.00	
	SK.82	127.00	2.00	0.20	0.10	0.60	0.10	0.10	155.30	8.00	7.40	0.20	0.10	0.20	0.10	1.00	0.50	12.10	
	SK.1	107.00	3.00	0.20	0.10	0.50	0.10	0.10	172.90	8.00	5.40	0.40	0.10	0.60	0.10	1.00	0.10	4.70	
	SK.64	32.00	1.00	0.20	0.10	0.50	0.10	0.10	484.90	8.00	1.20	0.40	0.20	0.60	0.10	1.00	0.10	3.30	
	SK.53	289.00	1.00	0.20	0.10	0.50	0.10	0.10	272.90	8.00	1.30	1.90	1.90	3.80	3.00	0.20	10.00	490.50	
	SK.43	1039.00	1.00	0.20	0.10	1.10	0.10	0.10	360.50	8.00	0.50	1.20	1.20	0.20	0.30	0.10	1.00	0.10	8.90
	SK.76	673.00	1.00	0.20	0.20	0.90	0.10	0.50	270.10	8.00	0.80	1.60	1.60	0.40	0.60	0.10	1.00	0.20	43.80
Shrub facies	SK.26	425.00	1.00	0.20	1.10	0.80	0.10	0.70	102.30	8.00	8.40	1.10	0.30	1.30	0.10	1.00	0.90	104.20	
	SK.45	449.00	2.00	0.20	0.10	1.50	0.40	0.10	71.90	16.00	12.90	3.50	1.70	1.30	0.10	9.00	0.10	248.40	
	SK.67	122.00	1.00	0.20	0.10	0.50	0.10	0.20	160.30	8.00	0.70	1.20	2.20	1.90	0.20	99.00	0.10	157.40	
	SK.7	2431.00	3.00	0.20	13.80	1.70	0.90	10.70	273.50	8.00	12.40	13.60	2.40	1.10	1.00	3.00	0.10	195.50	
Lithoclast facies	SK.55	208.00	1.00	1.10	29.10	2.80	2.30	23.20	176.60	12.00	39.00	35.30	4.00	3.00	2.00	7.00	2.00	361.20	
	SK.85	344.00	3.00	4.60	146.90	5.40	3.50	85.00	415.10	31.00	1.60	54.80	12.00	6.70	17.80	61.00	13.80	291.90	
Pisoid facies	SK.86	354.00	1.00	6.10	115.40	4.20	3.80	64.80	387.30	28.00	2.30	58.90	9.70	5.70	20.60	34.00	12.40	271.60	
	SK.40	259.00	3.00	0.30	1.40	1.10	0.60	5.30	407.70	18.00	0.50	13.80	17.50	1.10	1.20	2.00	0.50	17.80	
Recent hot water trav. sample	SK.35	393.00	4.00	0.20	2.60	0.80	0.10	1.60	455.50	16.00	0.50	8.90	12.80	0.10	5.50	2.00	0.10	17.80	
	SK.68	1293.00	1.00	0.20	0.10	0.50	0.10	0.10	1002.50	12.00	0.50	4.90	1.00	0.60	2.50	81.00	0.40	339.40	
Recent cold water trav. sample	SK.38	1209.00	3.00	0.20	0.30	0.50	0.10	0.10	1026.60	10.00	0.50	5.80	0.20	1.00	0.50	26.00	0.10	123.10	

Table 3 Rare-earth element compositions (in ppm) of travertine samples from the different facies in the Kavakköy Travertine

Facies type	Sample no.	La	Ce	Pr	Nd	Sm	Eu	Gd	Tb	Dy	Ho	Er	Tm	Yb	Lu	TOT/C	TOT/S
Crystalline crust facies	SK.48	0.2	0.2	0.02	0.3	0.05	0.02	0.06	0.01	0.1	0.04	0.03	0.01	0.05	0.01	12.31	0.02
	SK.74	0.1	0.2	0.03	0.3	0.05	0.02	0.05	0.01	0.05	0.02	0.03	0.01	0.05	0.01	12.16	0.02
	SK.10	0.1	0.2	0.02	0.3	0.05	0.02	0.08	0.01	0.06	0.02	0.07	0.01	0.05	0.01	12.46	0.02
	SK.59	0.1	0.1	0.06	0.3	0.05	0.02	0.05	0.01	0.07	0.02	0.03	0.01	0.05	0.01	12.19	0.03
	SK.82	0.1	0.1	0.02	0.7	0.05	0.02	0.05	0.01	0.05	0.02	0.03	0.01	0.05	0.01	12.34	0.02
	SK.1	0.1	0.1	0.02	0.3	0.05	0.02	0.05	0.01	0.05	0.02	0.03	0.01	0.05	0.01	12.18	0.02
	SK.64	0.1	0.1	0.02	0.3	0.05	0.07	0.05	0.01	0.05	0.02	0.03	0.01	0.05	0.01	12.44	0.11
	SK.53	0.4	2	0.2	1.1	0.2	0.08	0.4	0.05	0.29	0.08	0.24	0.01	0.14	0.02	12.46	0.02
	SK.43	0.3	0.1	0.02	0.3	0.05	0.02	0.05	0.01	0.05	0.02	0.03	0.01	0.05	0.01	12.2	0.02
	SK.76	0.2	0.5	0.05	0.6	0.05	0.02	0.06	0.01	0.13	0.02	0.03	0.01	0.05	0.01	12.81	0.02
Shrub facies	SK.26	0.1	0.2	0.03	1.5	0.07	0.07	0.05	0.01	0.05	0.02	0.03	0.01	0.05	0.01	12.31	0.02
	SK.45	0.3	0.2	0.02	0.3	0.07	0.02	0.21	0.04	0.05	0.02	0.03	0.01	0.14	0.23	12.05	0.02
	SK.67	0.1	0.7	0.05	0.4	0.05	0.02	0.11	0.01	0.09	0.02	0.13	0.01	0.07	0.01	12.41	0.02
	SK.7	2.7	5.5	0.62	2.8	0.41	0.04	0.4	0.07	0.39	0.07	0.21	0.03	0.15	0.03	11.94	0.06
Lithoclast facies	SK.55	4.9	10.1	1.08	4.3	0.76	0.16	0.64	0.1	0.6	0.12	0.38	0.05	0.35	0.06	11.25	0.02
	SK.85	15.9	28.6	3.74	11.5	1.86	0.49	2.45	0.29	1.76	0.36	0.87	0.11	1	0.14	10.74	0.05
Pisoid facies	SK.86	11.2	26.9	2.28	7.8	1.59	0.36	1.69	0.23	1.19	0.32	0.58	0.1	0.68	0.13	10.9	0.07
	SK.40	2.2	10.1	0.64	3.6	1.04	0.49	2.13	0.33	2.26	0.47	1.15	0.16	0.86	0.16	11.84	0.13
Recent hot water trav. sample	SK.35	2.2	3.5	0.32	3.2	1.11	0.2	1.61	0.26	1.98	0.33	0.67	0.25	0.61	0.1	11.66	0.11
	SK.68	0.2	0.3	0.02	0.3	0.06	0.02	0.1	0.01	0.05	0.05	0.04	0.03	0.14	0.02	12.31	0.04
Recent cold water trav. sample	SK.38	1	1.2	0.02	0.3	0.05	0.04	0.12	0.01	0.05	0.02	0.03	0.01	0.07	0.02	12.32	0.03

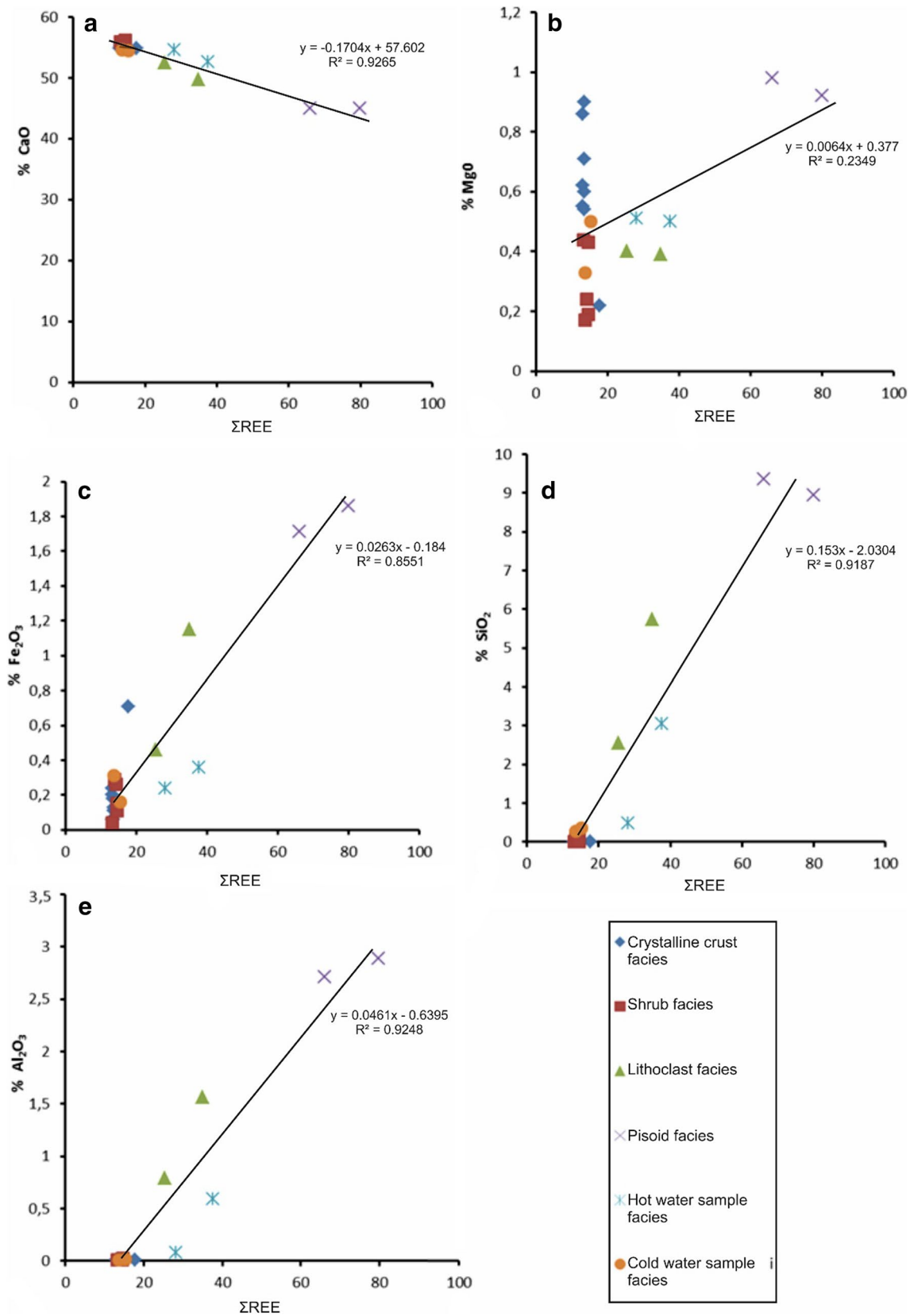


Fig. 11 Main oxide versus REE diagrams for recent and quaternary travertine facies in Kavakköy

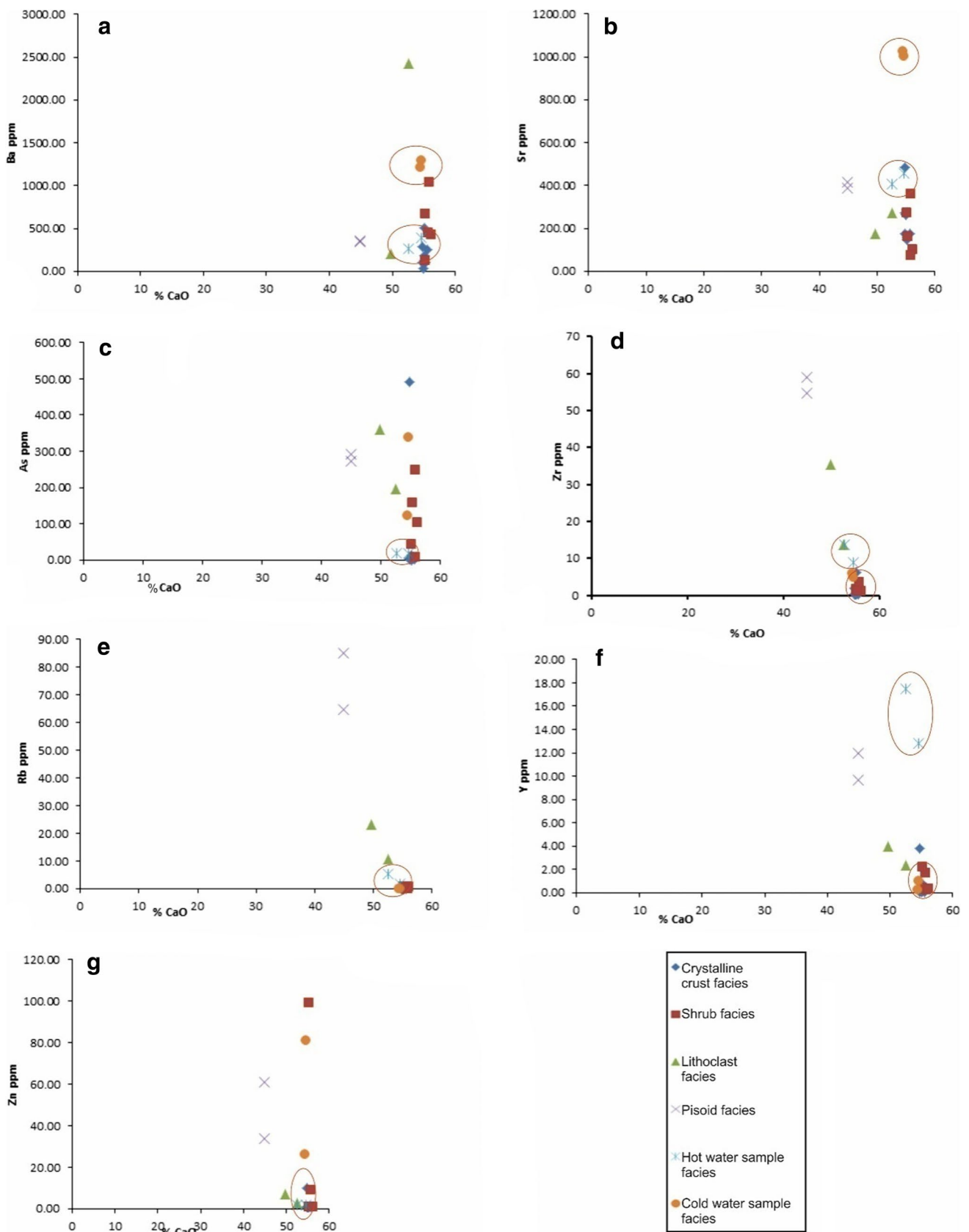


Fig. 12 CaO versus some of the REE diagrams for recent and quaternary travertine facies in Kavakköy

Table 4 Stable isotope compositions ($\delta^{18}\text{O}$ (VPDB), $\delta^{18}\text{O}$ (VSMOW) and $\delta^{13}\text{C}$ (VPDB)) and calculated $\delta^{13}\text{C}$ (VPDB) of travertine samples from the different facies in the Kavakköy Travertine

Sample no.	Facies type	Measured $\delta^{13}\text{C}$ (‰VPDB)	Calculated $\delta^{13}\text{C}$ (‰VPDB)	$\delta^{18}\text{O}$ (‰VPDB)	$\delta^{18}\text{O}$ (‰VSMOW)
SK 54	Crystalline crust facies	3.4	− 6.4	− 9.5	21.1
SK 1		3.5	− 6.3	− 10.9	19.7
SK 33		4.7	− 4.9	− 11.5	19.0
SK 41		5.6	− 3.8	− 10.6	20.0
SK 21		5.7	− 3.7	− 10.8	19.8
SK 10		5.9	− 3.4	− 10.0	20.6
SK 44		4.2	− 5.5	− 14.2	16.3
SK 15		4.5	− 5.1	− 13.7	16.8
SK 30		1.5	− 8.7	− 9.2	21.4
SK 5		4.1	− 5.6	− 13.9	16.6
SK 59		3.7	− 6.1	− 14.5	16.0
SK 80		0.2	− 10.3	− 9.5	21.1
SK 82		4.4	− 5.2	− 14.1	16.3
SK 22		4.4	− 5.2	− 13.8	16.6
SK 37		5.7	− 3.7	− 10.7	19.9
SK 20		4.6	− 5.0	− 13.9	16.6
SK 27		3.7	− 6.1	− 14.3	16.2
SK 81		5.9	− 3.4	− 10.5	20.1
SK 83		6.1	− 3.2	− 10.5	20.1
SK 14		3.8	− 5.9	− 14.6	15.8
SK 13		5.6	− 3.8	− 10.3	20.3
SK 46		4.6	− 5.0	− 13.4	17.1
SK 53		7.5	− 1.5	− 8.6	22.0
SK 48		3.8	− 5.9	− 14.5	15.9
SK 9		7.5	− 1.5	− 9.0	21.7
SK 79		6.4	− 2.8	− 8.5	22.1
SK 64		5.1	− 4.4	− 10.6	19.9
SK 6	Shrub facies	6.7	− 2.5	− 10.9	19.7
SK 12		3.6	− 6.2	− 14.5	16.0
SK 84		2.9	− 7.0	− 10.1	20.5
SK 23		5.5	− 3.9	− 10.1	20.5
SK 32		2.5	− 7.5	− 9.6	21.0
SK 16		5.6	− 3.8	− 10.8	19.7
SK 72		5.3	− 4.1	− 12.7	17.8
SK26		5.4	− 4.0	− 9.1	21.6
SK 77		3.4	− 6.4	− 9.2	21.4
SK 25		5.6	− 3.8	− 9.4	21.2
SK 28		5.1	− 4.4	− 8.9	21.7
SK 11		6.2	− 3.1	− 9.9	20.7
SK 57		5.5	− 3.9	− 11.2	19.4
SK 76		5.6	− 3.8	− 10.6	20.0
SK 43		5.6	− 3.8	− 12.0	18.6
SK 65	8.2	− 0.7	− 9.2	21.4	
SK 36	6.9	− 2.2	− 9.5	21.1	
SK 17	Lithoclast facies	5.6	− 3.8	− 10.0	20.6
SK 51		5.7	− 3.7	− 8.3	22.4
SK 86	Pisoid facies	7.4	− 1.6	− 7.8	22.8
SK 85		5.1	− 4.4	− 6.8	23.9

Table 4 (continued)

Sample no.	Facies type	Measured $\delta^{13}\text{C}$ (‰ VPDB)	Calculated $\delta^{13}\text{C}$ (‰ VPDB)	$\delta^{18}\text{O}$ (‰ VPDB)	$\delta^{18}\text{O}$ (‰ VSMOW)
SK 35	Recent hot water	5.4	− 4.0	− 13.5	17.0
SK 40	trav.	4.9	− 4.6	− 13.0	17.5
SK 38	Recent cold	8.0	− 0.9	− 8.7	21.9
SK 68	water trav.	7.3	− 1.7	− 8.7	21.9

of bedrock and karstic reservoir, tectonism, local climate, distance to the hydrothermal vents (Minissale et al. 2002; Pentecost 2005; Kele et al. 2011; Barilaro 2012; Özkul et al. 2014; Teboul et al. 2016). Negative $\delta^{18}\text{O}$ values are resulted from high saturation and high temperature. Similarly, light isotopes ($\delta^{16}\text{O}$ and $\delta^{12}\text{C}$) in the water may be removed from the system by biological activities and photosynthesis, leading to $\delta^{18}\text{O}$ and $\delta^{13}\text{C}$ enrichment in the water and the resultant carbonates (Barilaro 2012; Kele et al. 2011).

On the $\delta^{18}\text{O}$ (VPDB) versus $\delta^{13}\text{C}$ (VPDB) diagram, the recent samples from the hot water artesian site (39 °C) and those from the relatively cool spring site (19 °C) clustered into separate fields and, samples from crystalline crust facies are clustered around the field of hot water samples whereas other facies are scattered between these two fields (Fig. 13). The stable isotope values of the travertine at the Kavakköy region fall in the positive field on the diagram introduced by Gandin and Capezuoli (2008) (Fig. 14), which points that the Kavakköy Travertine, especially the crystalline crust facies, was deposited by relatively hot water.

The significant differences in the isotopic values of the recent travertines from two different sites having a water temperature of 19 °C and the other 39 °C are related to water circulation path and source of CO_2 (Table 4, Fig. 13). The travertine precipitated by water with a temperature of 19 °C

has comparatively short and shallow fluid flow paths and low (normal) heat flow and has CO_2 isotopic signatures, indicating a comparatively large quantity of CO_2 contribution from decarbonation of limestone. In contrast, the travertines formed by relatively hot water (39 °C) which were conductively heated during percolation through the thick Paleozoic–Cenozoic sequence have incorporated a comparatively large quantity of CO_2 derived from mantle sources. The Quaternary travertine deposits are scattered as mounds along the Seydişehir Fault Zone and are considered as being formed in relation with this fault zone. Therefore, the differences in stable isotope values in the Quaternary travertine are also interpreted to be the result of different water circulation paths.

The composition of isotopic carbon in travertine changes depending on the main source of CO_2 (Minissale, 2004). Panichi and Tongiorgi (1976) proposed an equation ($\delta^{13}\text{C}_{(\text{CO}_2)} = 1.2\delta^{13}\text{C}_{(\text{trav.})} - 10.5$) for recalculating the original $\delta^{13}\text{C}$ values of CO_2 from the measured $\delta^{13}\text{C}$ values in fossil travertines on the basis of data obtained from of Italian thermal springs and associated travertines. The studied travertine samples have high $\delta^{13}\text{C}$, between + 0.2 and + 8‰ (VPDB), and the calculated $\delta^{13}\text{C}$ values, using the Panichi and Tongiorgi's (1976) equation, range from − 10.3 to − 0.7‰ (VPDB). Both measured

Fig. 13 $\delta^{18}\text{O}$ (VPDB) values versus $\delta^{13}\text{C}$ (VPDB) values diagram of different facies types in the Kavakköy Travertine

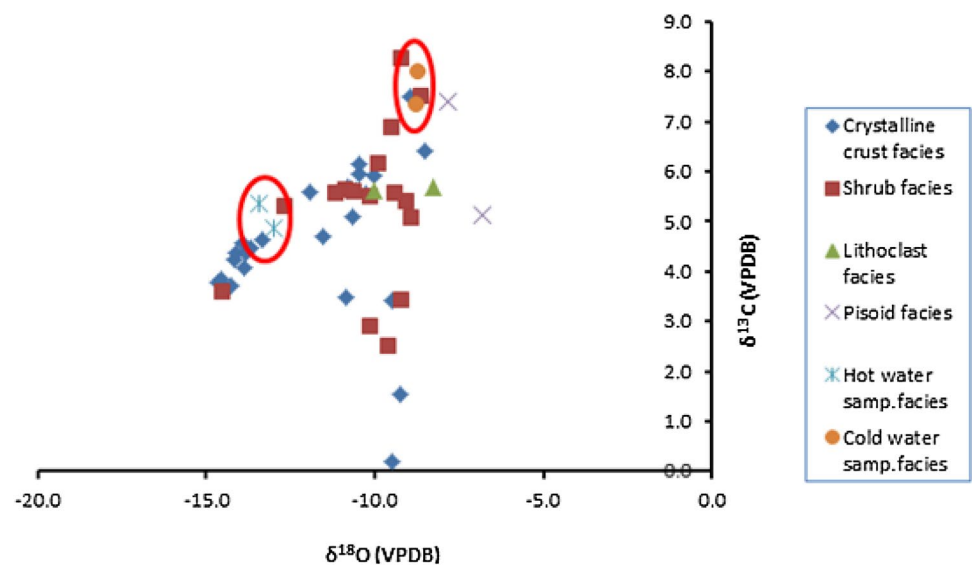


Fig. 14 Combined plot of $\delta^{18}\text{O}$ (VSMOW/VPDB) and $\delta^{13}\text{C}$ (VPDB) values derived from carbonates presently forming in terrestrial (travertine, calcareous tufa, speleothems) and marine (skeletal-oid sediments and pelagic muds) environments and from lithified marine limestones (Gandin and Capezzuoli 2008)

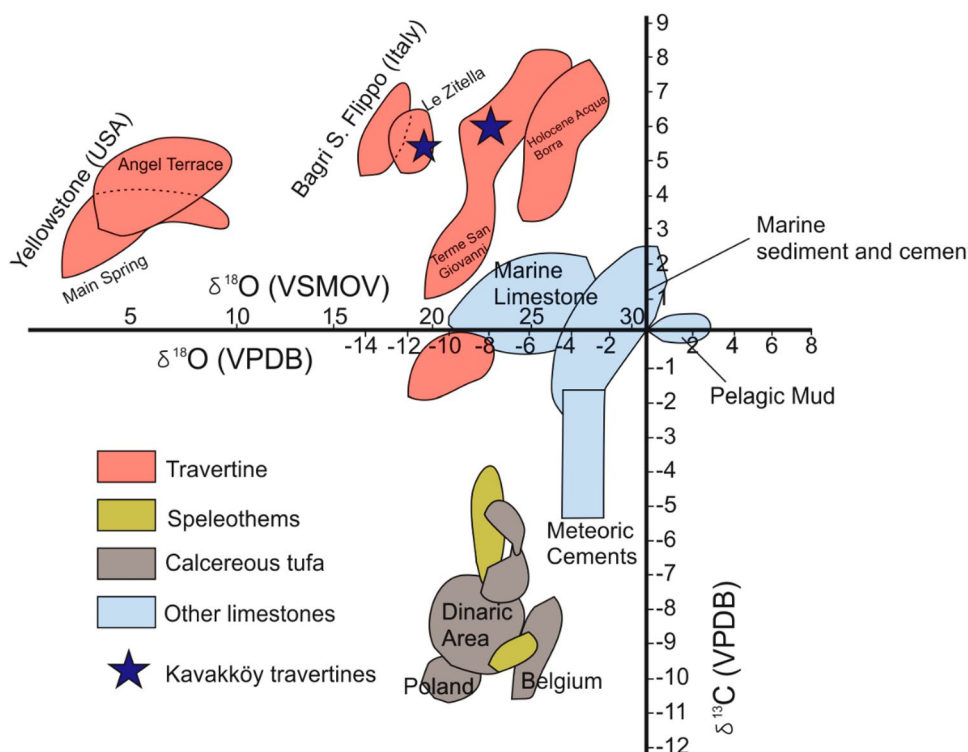
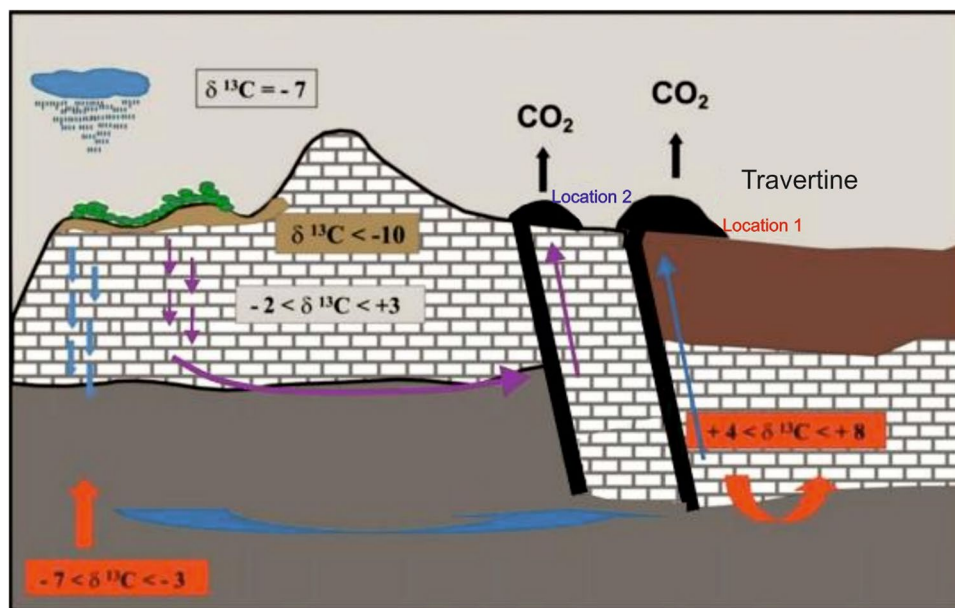


Fig. 15 A simplified model for sources of CO_2 in two recent travertine deposition sites in the study area (Location 1: hot water artesian well; Location 2: relatively cold spring). Modified after Minissale et al. (2002)



and calculated $\delta^{13}\text{C}$ values imply that the parent water of the Kavakköy Travertine was charged with CO_2 mainly from a deep mantle source (Figs. 15, 16; Minissale et al. 2002) with a little contribution from decarbonation of carbonate bedrocks (i.e., Paleozoic marbles and Miocene lacustrine carbonate).

Conclusions

1. In the study area, six different facies were determined from four Quaternary travertine mounds which are roughly aligned along the Seydişehir Fault Zone. These

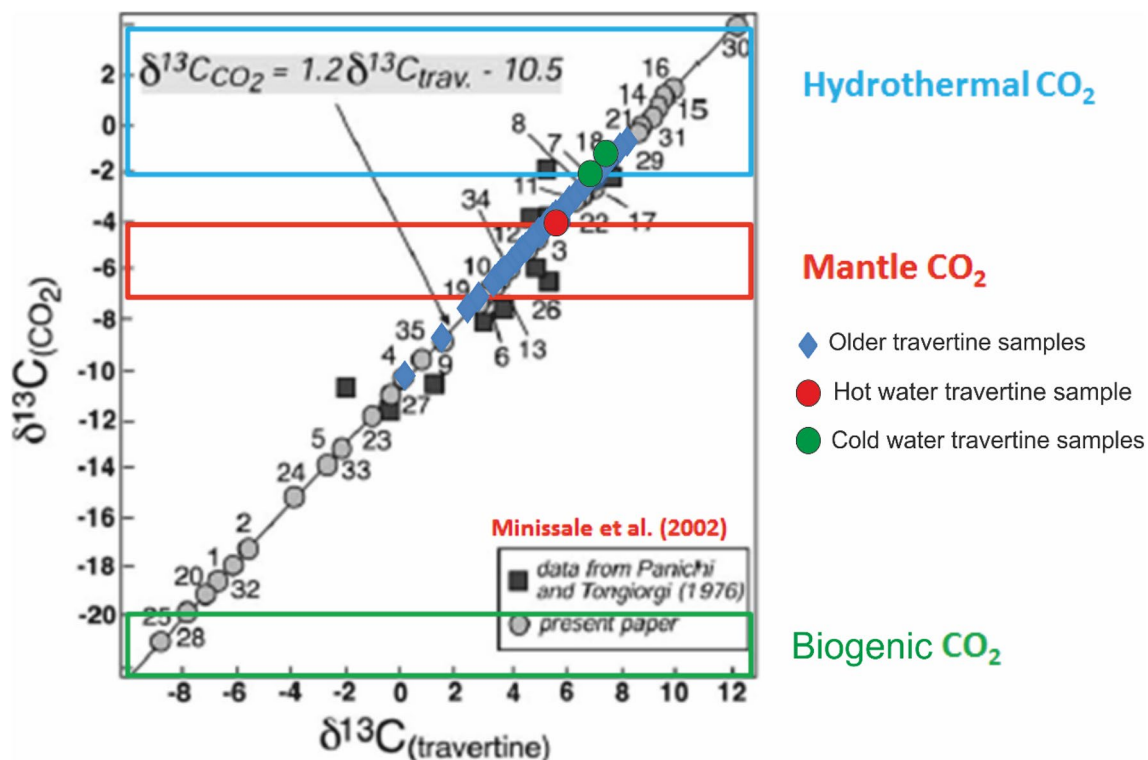


Fig. 16 $\delta^{13}\text{C}$ of CO_2 vs. $\delta^{13}\text{C}$ in CaCO_3 from actively depositing travertine areas (black squares) and $\delta^{13}\text{C}$ values of CO_2 ‘recalculated’ from $\delta^{13}\text{C}$ values (gray circles) of travertines according to the formula shown at the top of the diagram (Minissale et al. 2002)

are crystalline crust travertine, paper-thin raft travertine, coated bubble travertine, pisoid, lithoclast travertine, shrub travertine facies.

- The sedimentological, morphologic and geochemical characteristics of travertine facies point that the depositions took place in slope and depressional depositional systems.
- The $\delta^{18}\text{O}$ (VPDB) values indicate that the deposition of the facies in the Kavakköy Travertine is closely related to the water temperature. The crystalline crust facies was deposited by hot water, while shrub facies were deposited by relatively warm water.
- High $\delta^{13}\text{C}$ and the calculated $\delta^{13}\text{C}$ values of the Kavakköy Travertine has been explicated as that the majority of CO_2 was derived from a mantle source and that CO_2 contribution from metamorphism of limestone during thermometamorphic decarbonation of the Paleozoic and Mesozoic carbonate basement rocks was low.

Acknowledgements We are grateful to the Selcuk University Research Fund for the financial support (Project No. 12101018). Special thanks go to Prof. Dr. Ada Haynes from Tennessee Tech. University, USA for her contribution in improving the language of this manuscript. The critical comments on an earlier version of this manuscript by anonymous reviewers are greatly appreciated. This article is produced from Master Thesis of Seda Karaisaoglu supervised by Hükmü Orhan.

References

- Allen ET, Day AL (1935) Hot springs of the Yellowstone National Park. Carnegie Inst. Washington Pub. 466
- Altunel E (1996) Pamukkale Travertenlerinin morfolojik özellikleri, yaşları ve neotektonik önemleri. MTA Dergisi 118:47–64
- Baker G, Fiosticks AC (1951) Pisoliths, oololiths and calcareous growths in limestone caves at Port Campbell Victoria, Australia. J Sediment Petrol 21:85–104
- Bargar KE (1978) Geology and thermal history of Mammoth hot springs Yellowstone National Park Wyoming, U.S. Geol Surv Bull 1444:1–55
- Barilaro F (2012) The character and spatial distribution of Holocene and Pleistocene hydrothermal travertines Albegna Valley Southern Tuscany, Central Italy. Ph. D Thesis, Università Degli Studi Milano, p 176
- Broggi A, Capezzuoli E (2009) Travertine deposition and faulting: the fault related travertine fissure ridge at Terme S Giovanni, Rapolano Terme, Italy. Int J Earth Sci 98:931–947
- Casanova J (1986) East African Rift stromatolites, In: Frostick RW (ed) Sedimentation in the African Rifts, Geological Society of London Special Publication 25. London, pp 201–210
- Chafetz HS, Folk RL (1984) Travertines: depositional morphology and the bacterially constructed constituents. J Sediment Petrol 54:289–316
- Chafetz HS, Guidry SA (1999) Bacterial shrubs, crystal shrubs and ray-crystal shrubs: bacterial vs. abiotic precipitation. Sediment Geol 126:57–74
- Chafetz HS, Lawrence JR (1994) Stable isotopic variability within modern travertines. Geogr Phys Quat 48(3):257–273

- Chafetz HS, Rush PF, Utech NM (1991) Microenvironmental controls on mineralogy and habitat of CaCO_3 precipitates: an example from an active travertine system. *Sedimentology* 38:107–126
- Dandurand JL, Gout R, Hoefs J, Menschel G, Schott J, Usdowski E (1982) Kinetically controlled variations of major components and carbon and oxygen isotopes in a calcite-precipitating spring. *Chem Geol* 36:299–315
- Epstein S, Mayeda T (1953) Variation of ^{18}O content of waters from natural sources. *Geochim Cosmochim Acta* 4:89–103
- Folk RL, Chafetz HS (1983) Pisoliths (pisoids) in quaternary travertines of Tivoli, Italy. In: Peryt TM (ed) *Coated grains*. Springer, Berlin, pp 474–487
- Folk RL, Chafetz HS, Tiezzi PA (1985) Bizarre forms of depositional and diagenetic calcite in hot spring travertines, Central Italy: In: Schneiderman N, Harris PM (eds), *Carbonate cements*, Special Publication, Society Economic Paleontologist Mineralogist 36. Tulsa, pp 249–369
- Ford TD, Pedley HM (1996) A review of tufa and travertine deposits of the world. *Earth Sci Rev* 41:117–175
- Fouke BW, Farmer JD, Des Marais DJ, Pratt L, Sturchio NC, Burns PC, Discipulo MK (2000) Depositional facies and aqueous—solid geochemistry of travertine—depositing hot springs, Angel Terrace Mammoth Hot Springs Yellowstone National Park, U.S.A. *J Sediment Res* 70(3):565–585
- Gandin A, Capezzuoli E (2008) Travertine versus calcareous tufa: distinctive petrologic features and stable isotopes signatures. II Quaternario. *Ital J Quat Sci* 21(1B):125–136
- Guo L, Riding R (1992) Aragonite laminae in hot water travertine crusts, Rapolano Terme Italy. *Sedimentology* 39:1067–1079
- Guo L, Riding R (1994) Origin and diagenesis of quaternary travertine shrub fabrics, Rapolano Terme, central Italy. *Sedimentology* 41:499–520
- Guo L, Riding R (1998) Hot-spring travertine facies and sequences: late Pleistocene Rapolano Terme, Italy. *Sedimentology* 45:163–180
- Hancock PL, Chalmers RML, Altunel E, Çakır Z (1999) Travertines: using travertines in active fault studies. *J Struct Geol* 21:903–916
- Herman JS, Lorah MM (1987) CO_2 outgassing and calcite precipitation in Falling Spring Creek Virginia, U.S.A. *Chem Geol* 62:251–262
- Innocenti F, Mazzuoli R, Pasquare G, Radicati di Brozola F, Villari L (1975) The Neogene calcalkaline volcanism of Central Anatolia, Geochronological data on Kayseri-Niğde Area. *Geol Mag* 112(4):349–360
- Jacobson RL, Usdowski E (1975) Geochemical controls on a calcite precipitating spring. *Contrib Miner Petrol* 51:65–74
- Jones B, Renaut RW (2010) Calcareous spring deposits in continental settings. In: Alonso Zarza AM, Taner LH (eds) *Carbonates in continental settings: facies, environments, and processes: developments in sedimentology*, vol 61. Elsevier, Oxford, pp 177–224
- Kele S, Özkul M, Förizs I, Gökğöz A, Baykara MO, Alçiçek MC, Németh T (2011) Stable isotope geochemical study of Pamukkale travertines: new evidences of low-temperature non-equilibrium calcite-water fractionation. *Sediment Geol* 238:191–212
- Koçyiğit A (1984) Güneybatı Türkiye ve yakın dolayında levha içi yeni tektonik gelişim. *Türkiye Jeoloji Kurumu Bülteni* 27(1):1–16
- Koşun E (2012) Facies characteristic and depositional environments of Quaternary tufa deposits, Antalya, SW Turkey. *Carbonates Evaporites* 27(3):269–289
- Lorah MM, Herman JS (1988) The chemical evolution of a travertine-depositing stream: geochemical processes and mass transfer reaction. *Water Resour Res* 24:1541–1552
- McCrea JM (1950) On the isotopic chemistry of carbonates and a paleotemperature scale. *J Chem Phys* 18:849–857
- Minissale A (2004) Origin, transport and discharge of CO_2 in central Italy. *Earth Sci Rev* 66:89–141
- Minissale A, Kerrick DM, Magro G, Murrell MT, Paladini M, Rihs S, Vaselli O (2002) Geochemistry of quaternary travertines in the region north of Rome (Italy): structural, hydrologic and paleoclimatic implications. *Earth Planet Sci Lett* 203(2):709–728
- Orhan H, Kalan F (2015) Sedimentological characteristics of Quaternary Aydınçık tufa (Mersin- Türkiye). *Carbonates Evaporites* 30(4):451–459
- Özgül N (1976) Torosların bazı temel jeolojik özellikleri. *Türkiye Jeoloji Kurumu Bülteni* 19(1):65–78
- Özgül N (1997) Bozkır-Hadim-Taşkent (Orta Toroslar'ın Kuzey Kesimi) dolaylarında yer alan Tektono – Stratigrafik Birliklerin Stratigrafisi. *MTA Dergisi* 119:117–174
- Özkul M, Varol B, Alçiçek MC (2002) Denizli travertenlerinin petrografik özellikleri ve depolanma ortamları. *MTA Dergisi* 125:13–29
- Özkul M, Kele S, Gökğöz A, Shen CC, Jones B, Baykara MO, Förizs I, Németh T, Chang YW, Alçiçek MC (2013) Comparison of the quaternary travertine sites in the Denizli Extensional Basin based on their depositional and geochemical data. *Sediment Geol* 294:179–204
- Özkul M, Gökğöz A, Kele S, Baykara OM, Shen C, Chang Y, Kaya A, Hançer M, Aratman C, Akın T, Örüş Z (2014) Sedimentological and geochemical characteristics of fluvial travertine: a case from the eastern Mediterranean region. *Sedimentology* 61:291–318
- Panichi C, Tongiorgi E (1976) Carbon isotopic composition of CO_2 from springs, fumaroles, mofettes and travertines of central and southern Italy: a preliminary prospection method of geothermal areas. In: *Proceedings of the 2nd UN symposium on the development and use of geothermal resources*, San Francisco CA, 20–29 May 1975, pp 815–825
- Pedley HM (1990) Classification and environmental models of cool freshwater tufas. *Sediment Geol* 68:143–154
- Pentecost A (1990) The formation of travertine shrubs: mammoth hot springs, Wyoming. *Geol Mag* 127:159–168
- Pentecost A (2005) *Travertine*. Springer, Berlin, p 445
- Rainey DK, Jones B (2005) Radiating calcite dendrites- precursors for coated grain formation in the Fairmont Hot Springs Travertine, Canada. In: Özkul M, Yağız S, and Jones B (eds) *Proceedings of 1st International Symposium on Travertine September 21–25 2005, Denizli, Turkey*, pp 25–33
- Shen CC, Wu CC, Cheng H, Edwards RL, Hsieh YT, Gallet S, Chang CC, Li TY, Lam DD, Kano A, Hori M, Spötl C (2012) High-precision and high-resolution carbonate ^{230}Th dating by MC-ICP-MS with SEM protocols. *Geochim Cosmochim Acta* 99:71–86
- Spötl C, Vennemann TW (2003) Continuous-flow isotope ratio mass spectrometric analysis of carbonate minerals. *Rapid Commun Mass Spectr* 17:1004–1006
- Teboul PA, Durlot C, Gaucher EC, Virgone A, Girard JP, Curie J, Lopez B, Camoin GF (2016) Origins of elements building travertine and tufa: new perspectives provided by isotopic and geochemical tracers. *Sediment Geol* 334:97–114
- Zhang DD, Zhang Y, Zhu A, Cheng X (2001) Physical mechanism of river waterfall tufa (travertine) formation. *J Sediment Res* 71:205–216